



Preparation and characterization of Cp-functionalized cycloheptatrienyl–cyclopentadienyl titanium sandwich complexes (troticenes)

Alain C. Tagne Kuate, Swagat K. Mohapatra, Constantin G. Daniliuc, Peter G. Jones, Matthias Tamm*

Institut für Anorganische und Analytische Chemie, Technische Universität Braunschweig, Hagenring 30, 38106 Braunschweig, Germany

ARTICLE INFO

Article history:

Received 19 August 2011

Received in revised form

26 September 2011

Accepted 5 October 2011

Keywords:

Sandwich complexes

Cycloheptatrienyl complexes

Cyclopentadienyl ligands

Titanium

ABSTRACT

Cp-functionalized monotroticenes $[(\eta^7\text{-C}_7\text{H}_7)\text{Ti}(\eta^5\text{-C}_5\text{H}_4\text{E})]$ (**2**, E = Ph₂SiCl; **3**, E = *t*Bu₂SnCl; **12**, E = I) and bitroticenes $[(\eta^7\text{-C}_7\text{H}_7)\text{Ti}(\eta^5\text{-C}_5\text{H}_4)]_2\text{E}'$ (**5**, E' = PPh; **6**, E' = BN(SiMe₃)₂; **7**, E' = Cp₂Ti) were prepared by salt elimination metathesis between the monolithiated troticene $[(\eta^7\text{-C}_7\text{H}_7)\text{Ti}(\eta^5\text{-C}_5\text{H}_4\text{Li})]\cdot\text{pmdta}$ (**1b**) (pmdta = *N,N',N'',N'''*-pentamethyldiethylene-triamine) and the appropriate electrophile. The troticenylium-substituted zirconocene monochloride $[(\eta^7\text{-C}_7\text{H}_7)\text{Ti}(\eta^5\text{-C}_5\text{H}_4\text{ZrClCp}^*)_2]$ (Cp* = $\eta^5\text{-C}_5\text{Me}_5$) (**8**) and hafnocene ethoxide $[(\eta^7\text{-C}_7\text{H}_7)\text{Ti}(\eta^5\text{-C}_5\text{H}_4\text{Hf}(\text{OEt})\text{Cp}_2)]$ (Cp = $\eta^5\text{-C}_5\text{H}_5$) (**11**), and the heterobimetallic μ -oxo complexes $[(\eta^7\text{-C}_7\text{H}_7)\text{Ti}(\eta^5\text{-C}_5\text{H}_4\text{MCp}_2)]_2\text{O}$ (**9**, M = Zr; **10**, M = Hf) were obtained instead of the expected zircona- and hafna[1]troticenophanes by reaction of the dilithiated troticene $[(\eta^7\text{-C}_7\text{H}_6\text{Li})\text{Ti}(\eta^5\text{-C}_5\text{H}_4\text{Li})]\cdot\text{pmdta}$ (**1a**) with $[\text{Cp}_2\text{MCl}_2]$ (M = Zr, Hf) or $[\text{Cp}^*\text{ZrCl}_2]$ in stoichiometric amounts. These compounds were characterized by single crystal X-ray diffraction analyses and, in the case of **2**, **3**, **5**–**7**, **9**, **10** and **12**, also by elemental analyses and ¹H, ¹³C and ¹¹⁹Sn NMR spectroscopy. Exposure of the troticenylium organotin chloride **3** to moisture resulted in its partial hydrolysis and formation of the organostannoxane-bridged bitroticene **4**, while palladium-catalyzed Negishi C–C cross-coupling reaction between the troticenylium chloride $[(\eta^7\text{-C}_7\text{H}_7)\text{Ti}(\eta^5\text{-C}_5\text{H}_4\text{ZnCl})]$ (**13**) and the iodotroticene **12** or iodobenzene (PhI) led to the fulvalene complexes $[(\eta^7\text{-C}_7\text{H}_7)\text{Ti}(\eta^5\text{-C}_5\text{H}_4)]_2$ (**14**) and $[(\eta^7\text{-C}_7\text{H}_7)\text{Ti}(\eta^5\text{-C}_5\text{H}_4\text{Ph})]$ (**15**). Compound **4** displays an unsymmetrical structure with the troticenylium fragments *cis* with respect to the Sn–O–Sn core, whereas compound **14** is centrosymmetrically *trans* oriented.

© 2011 Elsevier B.V. All rights reserved.

1. Introduction

The discovery of bis(η^5 -cyclopentadienyl)iron(II) (ferrocene) and the elucidation of its sandwich structure by Fischer and Wilkinson [1,2] in the 1950s prepared the ground for the development of modern organometallic chemistry [3]. Today, ferrocene-based compounds have become an important chemical subclass because of favorable chemical and physical properties that include high thermal stability, specific and unique geometries, stability toward moisture and oxygen and the ability to undergo reversible redox reactions. Furthermore, the metalation of one or both cyclopentadienyl rings with organolithium reagents followed by the addition of electrophiles has led to a wider spectrum of functionalized ferrocenes that have found numerous applications in diverse areas such as electrochemistry [4], homogeneous catalysis [5], polymer and medicinal chemistry [6,7], ligand design [8] and materials science [9].

In contrast, the modification of other sandwich complexes is significantly less well developed and, for instance, mixed cycloheptatrienyl–cyclopentadienyl (Cht–Cp) sandwich complexes have only rarely been employed, even though group 4–6 complexes of the type $[(\eta^7\text{-C}_7\text{H}_7)\text{M}(\eta^5\text{-C}_5\text{H}_5)]$ (M = Ti, Zr, Hf, V, Nb, Ta, Cr, Mo, W) have been known for a long time [10,11]. To date, metalation has only been achieved for the 3d-transition metal complexes **I** (Fig. 1), troticene (M = Ti), trovacene (M = V) and trochrocene (M = Cr), and the first report on the dilithiation of troticene using *n*BuLi/tmeda (tmeda = *N,N,N',N''*-tetramethylethylenediamine) dates back to 1974 [12]. Optimization of this method provided access to a number of difunctionalized troticene derivatives of the type $[(\eta^7\text{-C}_7\text{H}_6\text{E})\text{Ti}(\eta^5\text{-C}_5\text{H}_4\text{E})]$ (**II**) [13–15] and, in our hands, to *ansa*-Cht–Cp complexes such as the sila- and germa[1]troticenophanes of type **III** (Fig. 1) [16–19]. In a similar fashion, dilithiated trovacene and trochrocene can be obtained, allowing the preparation of related bora- and sila[1]trovacenophanes [17,20,21], bora-, sila- and germa[1]trochrocenophanes [21,22,23], dibora- and disila[2]trovacenophanes [20,21] and dibora- and disila[2]trochrocenophanes [24,22]. Recent developments involved the use of *n*BuLi/pmdta (pmdta = *N,N',N'',N'''*-pentamethyldiethylenetriamine), affording

* Corresponding author. Tel.: +49 0 531 391 5309; fax: +49 0 531 391 5387.

E-mail address: m.tamm@tu-bs.de (M. Tamm).

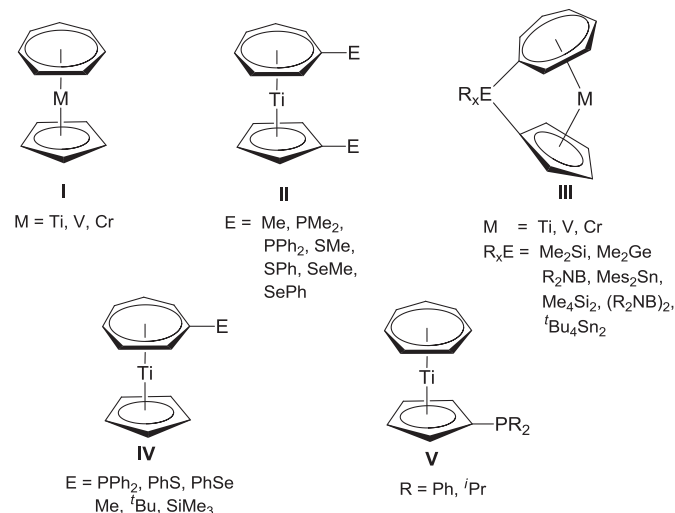


Fig. 1. Functionalized cycloheptatrienyl–cyclopentadienyl sandwich complexes.

$[(\eta^7\text{-C}_7\text{H}_6\text{Li})\text{Ti}(\eta^5\text{-C}_5\text{H}_4\text{Li})] \cdot \text{pmdta}$ (**1a**), which can conveniently be isolated as a dimeric species in crystalline form (Fig. 2) and subsequently be employed for the preparation of trocicenyl diphosphanes such as $[(\eta^7\text{-C}_7\text{H}_6\text{PPh}_2)\text{Ti}(\eta^5\text{-C}_5\text{H}_4\text{PPh}_2)]$ (dppti) [25] and various boron-, silicon- and tin-bridged [1]- and [2]trocicenophanes [26].

The *n*BuLi/pmdta combination not only proved suitable for the dilithiation of trocicene, but also allowed its selective monolithiation [25]. In agreement with earlier reports, the reaction of trocicene with 1 eq. of *n*BuLi in diethyl ether initially results in the kinetically controlled formation of $[(\eta^7\text{-C}_7\text{H}_6\text{Li})\text{Ti}(\eta^5\text{-C}_5\text{H}_5)]$, which can be used for the preparation of Cht-functionalized trocicenes (**IV**) [15,25,27]. After prolonged reaction times, however, the thermodynamically favored Cp-metalated lithiotrocicene is formed. More conveniently, monolithiation with the same regioselectivity can be achieved in much shorter reaction times by the use of *n*BuLi/pmdta in hexane. The resulting $[(\eta^7\text{-C}_7\text{H}_7)\text{Ti}(\eta^5\text{-C}_5\text{H}_4\text{Li})] \cdot \text{pmdta}$ (**1b**) can be isolated in high yield as a dark green crystalline material (Fig. 2), which was treated with ClPPh₂ to obtain the trocicenyl monophosphane $[(\eta^7\text{-C}_7\text{H}_7)\text{Ti}(\eta^5\text{-C}_5\text{H}_4\text{PPh}_2)]$ [25]. This direct method for the preparation of trocicenes of type **V** (Fig. 1) is clearly superior and also more versatile than our previously established route, which involved the preparation of the half-sandwich complexes $[(\eta^5\text{-C}_5\text{H}_4\text{PR}_2)\text{TiCl}_3]$ (R = Ph, ⁱPr), followed by reduction with magnesium in the presence of cycloheptatriene [28].

With the key intermediate **1b** in hand, a great variety of functional groups can now be attached selectively at the five-membered ring, and in this contribution, we wish to report our results on the exploitation of **1b** for the synthesis of a wide range of Cp-functionalized monotrocicenes and bridged bitrocicenes. In addition, several reactions are described in which the use of the dilithiotrocicene **1a** also resulted in the formation of Cp-functionalized trocicenes.

2. Experimental section

2.1. General procedures

All reactions were performed in a glove box under a dry atmosphere of argon (MBraun 200B) or on a high-vacuum line using Schlenk techniques. Commercial grade solvents were purified by use of a solvent purification system from MBraun GmbH and stored over molecular sieves (4 Å). Tetrahydrofuran was additionally dried over sodium/benzophenone, distilled, degassed and stored under

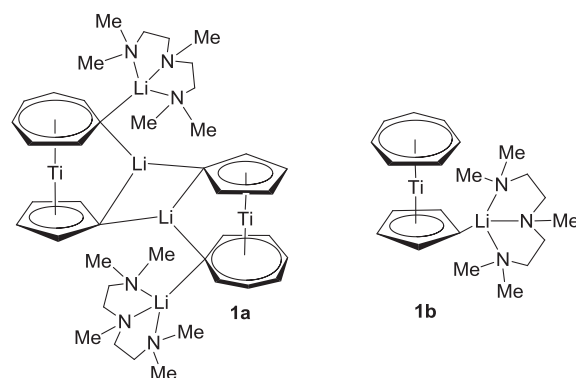


Fig. 2. Mono- and dilithiated cycloheptatrienyl–cyclopentadienyl titanium complexes.

argon. Ph₂SiCl₂, ^tBu₂SnCl₂, $[(\eta^5\text{-C}_5\text{H}_5)_2\text{TiCl}_2]$, 1,2-diiodoethane, ZnCl₂ and iodobenzene were purchased from Sigma–Aldrich Co. and used as received. Published procedures were used to prepare $[(\eta^7\text{-C}_7\text{H}_6\text{Li})\text{Ti}(\eta^5\text{-C}_5\text{H}_4\text{Li})] \cdot \text{pmdta}$ (**1a**), $[(\eta^7\text{-C}_7\text{H}_7)\text{Ti}(\eta^5\text{-C}_5\text{H}_4\text{Li})] \cdot \text{pmdta}$ (**1b**) [25], $[(\eta^5\text{-C}_5\text{H}_5)_2\text{ZrCl}_2]$ [29a], $[(\eta^5\text{-C}_5\text{H}_5)_2\text{HfCl}_2]$ [29a], $[(\eta^5\text{-C}_5\text{Me}_5)_2\text{ZrCl}_2]$ [29a], Cl₂BN(SiMe₃)₂ [29b,c] and [Pd(dppf)Cl₂] (dppf = 1,1'-bis(diphenylphosphanyl)ferrocene) [29d]. NMR spectra were recorded on Bruker DPX 200, DRX 400 and AV 300 devices. Chemical shifts (δ) are reported in ppm and referenced to tetramethylstannane (¹¹⁹Sn), tetramethylsilane (¹H, ¹³C) and 85% H₃PO₄ (³¹P). Coupling constants (*J*) are reported in Hertz (Hz) and splitting patterns are indicated as s (singlet), d (doublet), t (triplet) and m (multiplet). Elemental analyses (C, H, N) were performed by combustion and gas chromatographic analysis with an Elementar Vario MICRO elemental analyzer. UV/vis spectra were recorded on a Shimadzu UV Mini 1240 UV/vis photometer. Electron ionization mass spectrometry (EI-MS) was performed on a Finnigan MAT 90 device.

2.2. Synthesis and characterization of $[(\eta^7\text{-C}_7\text{H}_7)\text{Ti}(\eta^5\text{-C}_5\text{H}_4\text{SiPh}_2\text{Cl})]$ (**2**)

A solution of Ph₂SiCl₂ (0.116 g, 0.456 mmol) in hexane (10 mL) was added dropwise to a suspension of **1b** (0.175 g, 0.456 mmol) in hexane (15 mL) at -78°C . The mixture was slowly allowed to reach ambient temperature, and stirring was continued overnight. The color of the suspension changed from green to light blue. The solid was filtered off and washed repeatedly with hexane. Toluene (10 mL) was added, and the solution was filtered to remove LiCl. Drying under vacuum afforded 0.150 g (84%) of pure **2** as a blue solid. Anal. Calcd. (%) for C₂₄H₂₁ClSiTi (420.83): C 68.49; H 5.02. Found: C 67.65; H 5.05. ¹H NMR (200 MHz, C₆D₆, 297 K) δ : 7.67–6.99 (m, 10H, Ph), 5.37 (s, 7H, C₇H₇), 5.29 (t, *J*_{H–H} = 5.3 Hz, 2H, C₅H₄), 5.11 (t, *J*_{H–H} = 5.3 Hz, 2H, C₅H₄). ¹³C{¹H} NMR (50.3 MHz, C₆D₆, 297 K) δ : 135.5 (s, C₆H₅), 135.2 (s, *i*-C₆H₅), 131.3 (s, C₆H₅), 128.8 (s, C₆H₅), 104.5 (C₅H₄), 102.5 (s, *i*-C₅H₄), 101.3 (s, C₅H₄), 87.8 (s, C₇H₇).

2.3. Synthesis and characterization of $[(\eta^7\text{-C}_7\text{H}_7)\text{Ti}(\eta^5\text{-C}_5\text{H}_4\text{Sn}^t\text{Bu}_2\text{Cl})]$ (**3**) and $[(\eta^7\text{-C}_7\text{H}_7)\text{Ti}(\eta^5\text{-C}_5\text{H}_4\text{Sn}^t\text{Bu}_2)_2\text{O}]$ (**4**)

A solution of ^tBu₂SnCl₂ (0.118 g, 0.390 mmol) in hexane (10 mL) was added dropwise to a suspension of **1b** (0.136 g, 0.355 mmol) in hexane (12 mL) at -78°C . The mixture was allowed to warm up slowly to ambient temperature, and stirring was continued overnight, whereby the green suspension turned into a blue-green solution. After filtration over Celite, the solvent was removed *in vacuo* to give a green residue. Recrystallization from pentane

at $-30\text{ }^{\circ}\text{C}$ gave 0.070 mg (42%) of pure **3** as blue-green crystalline solid. Anal. Calcd. (%) for $\text{C}_{20}\text{H}_{29}\text{ClSnTi}$ (471.47): C 50.95; H 6.20. Found: C 51.30; H 6.34. ^1H NMR (400 MHz, C_6D_6 , 297 K) δ : 5.44 (s, 7H, C_7H_7), 5.21 (t, $J_{\text{H-H}} = 5.1$ Hz, $^3J_{\text{H-Sn}} = 12.8/17.9$ Hz, 2H, $\alpha\text{-C}_5\text{H}_4$), 5.11 (t, $J_{\text{H-H}} = 5.1$ Hz, $^3J_{\text{H-Sn}} = 12.3/17.3$ Hz, 2H, $\beta\text{-C}_5\text{H}_4$). $^{13}\text{C}\{^1\text{H}\}$ NMR (100.7 MHz, C_6D_6 , 297 K) δ : 103.7 (s, $i\text{-C}_5\text{H}_4$), 103.4 (s, $^2J_{\text{C-Sn}} = 43.8$ Hz, $\alpha\text{-C}_5\text{H}_4$), 100.0 (s, $^3J_{\text{C-Sn}} = 40.0$ Hz, $\beta\text{-C}_5\text{H}_4$), 87.0 (s, C_7H_7), 36.0 (s, $^1J_{\text{C-Sn}} = 402.3/423.7$ Hz, C_q), 30.2 (s, CH_3). $^{119}\text{Sn}\{^1\text{H}\}$ NMR δ : 30.3.

Compound **4** was obtained as a hydrolyzed by-product of **3** during our attempt to recrystallize the remaining crude product from hexane by slow evaporation at room temperature. Yield: 11 mg (3.5%). Anal. Calcd. (%) for $\text{C}_{40}\text{H}_{58}\text{OSn}_2\text{Ti}_2$ (888.04): C 54.10; H 6.58. Found: C 54.61; H 6.23.

2.4. Synthesis and characterization of $[(\eta^7\text{-C}_7\text{H}_7)\text{Ti}(\eta^5\text{-C}_5\text{H}_4)]_2\text{PPh}$ (**5**)

A solution of PhPCl_2 (0.055 g, 0.248 mmol) in hexane (8 mL) was added dropwise to a suspension of **1b** (0.190 g, 0.495 mmol) in hexane (20 mL) at $-78\text{ }^{\circ}\text{C}$. The mixture was allowed to warm up slowly to ambient temperature, and stirring was continued overnight. The color of the suspension changed from green to dark green. The solid was filtered and washed repeatedly with hexane. Toluene (10 mL) was added and the solution was filtered to remove LiCl. Drying under vacuum afforded 0.090 g (72%) of pure **5** as a green solid. Anal. Calcd. (%) for $\text{C}_{30}\text{H}_{27}\text{PTi}_2$ (514.24): C 70.07; H 5.29. Found: C 69.20; H 5.56. ^1H NMR (200 MHz, C_6D_6 , 297 K) δ : 7.50–6.99 (m, 5H, Ph), 5.44 (s, 7H, C_7H_7), 5.13 (t, $J_{\text{H-H}} = 5.0$ Hz, 2H, C_5H_4), 4.98 (t, $J_{\text{H-H}} = 5.0$ Hz, 2H, C_5H_4). $^{13}\text{C}\{^1\text{H}\}$ NMR (50.3 MHz, C_6D_6 , 297 K) δ : 135.3 (d, $^1J_{\text{C-P}} = 23.2$ Hz, $i\text{-C}_6\text{H}_5$), 131.8 (d, $^3J_{\text{C-P}} = 7.0$ Hz, $m\text{-C}_6\text{H}_5$), 129.9 (d, $^2J_{\text{C-P}} = 11.2$ Hz, $o\text{-C}_6\text{H}_5$), 126.2 (s, $p\text{-C}_6\text{H}_5$), 103.2 (d, $^1J_{\text{C-P}} = 17.0$ Hz, $i\text{-C}_5\text{H}_4$), 101.8 (d, $^2J_{\text{C-P}} = 9.8$ Hz, $\alpha\text{-C}_5\text{H}_4$), 100.2 (d, $^2J_{\text{C-P}} = 2.8$ Hz, $\beta\text{-C}_5\text{H}_4$), 88.0 (s, C_7H_7). $^{31}\text{P}\{^1\text{H}\}$ NMR (81 MHz, C_6D_6 , 297 K) δ : -29.2 (s).

2.5. Synthesis and characterization of $[(\eta^7\text{-C}_7\text{H}_7)\text{Ti}(\eta^5\text{-C}_5\text{H}_4)]_2\text{BN}(\text{SiMe}_3)_2$ (**6**)

A solution of $\text{Cl}_2\text{BN}(\text{SiMe}_3)_2$ (0.064 g, 0.265 mmol) in hexane (5 mL) was added dropwise to a suspension of **1b** (0.205 g, 0.534 mmol) in hexane (15 mL) at $-78\text{ }^{\circ}\text{C}$. The mixture was allowed to warm up slowly to ambient temperature, and stirring was continued overnight. The green suspension turned into a green solution. After filtration over Celite, the solvent was removed *in vacuo* to give a green residue. The solid was washed with cold hexane and dried under vacuum, affording 0.105 g (69%) of pure **6** as a green solid. Anal. Calcd. (%) for $\text{C}_{30}\text{H}_{40}\text{BNSi}_2\text{Ti}_2$ (577.36): C 62.41; H 6.98. N 2.43 Found: C 61.71; H 6.71; N 2.81 ^1H NMR (200 MHz, C_6D_6 , 297 K) δ : 5.51 (s, 14H, C_7H_7), 5.36 (t, $J_{\text{H-H}} = 5.3$ Hz, 4H, C_5H_4), 5.14 (t, $J_{\text{H-H}} = 5.3$ Hz, 4H, C_5H_4). $^{13}\text{C}\{^1\text{H}\}$ NMR (50.3 MHz, C_6D_6 , 297 K) δ : 105.3 (s, C_5H_4), 100.9 (s, $i\text{-C}_5\text{H}_4$), 100.3 (s, C_5H_4), 87.3 (s, C_7H_7). $^{11}\text{B}\{^1\text{H}\}$ NMR (96.29; Hz, C_6D_6 , 297 K) δ : 36.7 (bs).

2.6. Synthesis and characterization of $[(\eta^7\text{-C}_7\text{H}_7)\text{Ti}(\eta^5\text{-C}_5\text{H}_4)]_2\text{Ti}(\eta^5\text{-C}_5\text{H}_5)_2$ (**7**)

A solution of $[(\eta^5\text{-C}_5\text{H}_5)_2\text{TiCl}_2]$ (0.060 g, 0.260 mmol) in hexane (10 mL) was added dropwise to a suspension of **1b** (0.200 g, 0.520 mmol) in hexane (20 mL) at $-78\text{ }^{\circ}\text{C}$. The mixture was slowly allowed to reach ambient temperature, and stirring was continued overnight. After removing the solvent, the residue was extracted with toluene, followed by evaporation of the solvent. The resulting purple solid was washed with hexane and dried under vacuum affording 0.085 g (56%) of pure **7** as a dark purple powder. Anal.

Calcd. (%) for $\text{C}_{34}\text{H}_{32}\text{Ti}_3$ (584.22): C 69.90; H 5.52. Found: C 68.34; H 6.04. ^1H NMR (200 MHz, C_6D_6 , 297 K) δ : 5.96 (s, 10H, C_5H_5), 5.31 (s, 14H, C_7H_7), 5.0 (t, $J_{\text{H-H}} = 5.0$ Hz, 4H, C_5H_4), 4.79 (t, $J_{\text{H-H}} = 5.0$ Hz, 4H, C_5H_4). $^{13}\text{C}\{^1\text{H}\}$ NMR (50.3 MHz, C_6D_6 , 297 K) δ : 112.9 (s, C_5H_5), 110.2 (s, C_5H_4), 108.0 (s, $i\text{-C}_5\text{H}_4$), 98.3 (s, C_5H_4), 86.9 (s, C_7H_7).

2.7. Synthesis and characterization of $[(\eta^7\text{-C}_7\text{H}_7)\text{Ti}(\eta^5\text{-C}_5\text{H}_4\text{ZrCl}(\eta^5\text{-C}_5\text{Me}_5)_2)]$ (**8**)

A solution of $[(\eta^5\text{-C}_5\text{Me}_5)_2\text{ZrCl}_2]$ (0.177 g, 0.409 mmol) in THF (15 mL) was added dropwise to a suspension of **1a** (0.144 g, 0.372 mmol) in hexane (15 mL) at $-78\text{ }^{\circ}\text{C}$. The mixture was slowly allowed to reach ambient temperature, and stirring was continued overnight. The green suspension turned into a dark brown solution. After filtration over Celite, the solvent was removed *in vacuo* to give a brown residue. The latter was then dissolved in hexane. Slow evaporation of the solvent afforded a few yellow-green crystals of **8** (0.007 g, 3.1%) suitable for an X-ray diffraction analysis. ^1H NMR (200 MHz, THF- d_8 , 297 K) δ : 5.58 (t, $J_{\text{H-H}} = 4.0$ Hz 2H, C_5H_4), 5.41 (s, 2H, C_5H_4), 4.98 (t, $J_{\text{H-H}} = 4.0$ Hz, 2H, C_5H_4).

2.8. Synthesis and characterization of $[(\eta^7\text{-C}_7\text{H}_7)\text{Ti}(\eta^5\text{-C}_5\text{H}_4\text{Zr}(\eta^5\text{-C}_5\text{H}_5)_2)]_2\text{O}$ (**9**)

A solution of $[(\eta^5\text{-C}_5\text{H}_5)_2\text{ZrCl}_2]$ (0.249 g, 0.850 mmol) in THF (20 mL) was added dropwise to a suspension of **1a** (0.301 g, 0.773 mmol) in hexane (20 mL) at $-78\text{ }^{\circ}\text{C}$. The color of the suspension turned instantaneously from green to light green. The mixture was allowed to warm up to $-30\text{ }^{\circ}\text{C}$, and the solid was isolated by filtration and dried *in vacuo*. The solid was dissolved in CH_2Cl_2 (10 mL) and filtered through Celite to remove LiCl. Evaporation of the solvent gave 0.201 g (30.1%) of pure **9** as a light green solid. Anal. Calcd. (%) for $\text{C}_{44}\text{H}_{42}\text{OTi}_2\text{Zr}_2$ (864.99): C 61.10; H 4.89. Found: C 60.24; H 5.10. ^1H NMR (200 MHz, CD_2Cl_2 , 297 K) δ : 5.83 (s, 20H, C_5H_5), 5.56 (t, $J_{\text{H-H}} = 4.8$ Hz, 4H, C_5H_4), 5.43 (t, 14H, C_7H_7). $^{13}\text{C}\{^1\text{H}\}$ NMR (100.68 MHz, CD_2Cl_2 , 297 K) δ : 147.3 (s, $i\text{-C}_5\text{H}_4$), 111.8 (s, C_5H_4), 111.1 (s, C_5H_5), 101.0 (s, C_5H_4), 85.5 (s, C_7H_7).

2.9. Synthesis and characterization of $[(\eta^7\text{-C}_7\text{H}_7)\text{Ti}(\eta^5\text{-C}_5\text{H}_4\text{Hf}(\eta^5\text{-C}_5\text{H}_5)_2)]_2\text{O}$ (**10**) and $[(\eta^7\text{-C}_7\text{H}_7)\text{Ti}(\eta^5\text{-C}_5\text{H}_4\text{Hf}(\eta^5\text{-C}_5\text{H}_5)_2\text{OEt})]$ (**11**)

A solution of $[(\eta^5\text{-C}_5\text{H}_5)_2\text{HfCl}_2]$ (0.140 g, 0.367 mmol) in THF (15 mL) was added dropwise to a suspension of **1a** (0.130 g, 0.334 mmol) in hexane (15 mL) at $-78\text{ }^{\circ}\text{C}$. The color of the suspension turned instantaneously from green to light green. The mixture was allowed to warm up to $-30\text{ }^{\circ}\text{C}$, and the precipitate was filtered off and dried *in vacuo*. This solid was dissolved in toluene (10 mL) and filtered to remove LiCl. Evaporation of the solvent gave 0.102 g (34.7%) of pure **10** as a light green solid. Anal. Calcd. (%) for $\text{C}_{44}\text{H}_{42}\text{Hf}_2\text{OTi}_2$ (1039.52): C 50.84; H 4.07. Found: C 51.28; H 4.34. ^1H NMR (300.13 MHz, THF- d_8 , 297 K) δ : 6.31 (s, 20H, C_5H_5), 5.41 (s, 14H, C_7H_7), 5.25 (t, $J_{\text{H-H}} = 4.7$ Hz, 8H, C_5H_4), 5.10 (t, $J_{\text{H-H}} = 4.7$ Hz, 8H, C_5H_4). $^{13}\text{C}\{^1\text{H}\}$ NMR (75.4 MHz, THF- d_8 , 297 K) δ : 126.0 (s, $i\text{-C}_5\text{H}_4$), 112.6 (s, C_5H_4), 109.1 (s, C_5H_5), 98.0 (s, C_5H_4), 85.9 (s, C_7H_7).

After separation of the light green solid, the filtrate was evaporated *in vacuo* to give a brown residue. Attempts to recrystallize this brown residue by slow evaporation of its diethyl ether solution afforded a small quantity of **11** as green crystals suitable for an X-ray diffraction analysis.

2.10. Synthesis and characterization of $[(\eta^7\text{-C}_7\text{H}_7)\text{Ti}(\eta^5\text{-C}_5\text{H}_4)]$ (**12**)

A solution of 1,2-diiodoethane (0.40 g, 1.40 mmol) in hexane (20 mL) was added dropwise to a suspension of **1b** (0.450 g, 1.170 mmol) in hexane (10 mL) at $-78\text{ }^{\circ}\text{C}$. The reaction mixture was

slowly warmed up to room temperature, and stirring was continued overnight. The color of the suspension turned from dark green to green. The solid was isolated by filtration, washed several times with hexane until the solution became colorless and dried *in vacuo*. The solid was then dissolved in toluene (15 mL) and filtered through Celite to remove LiCl. Repeated crystallization from toluene at $-30\text{ }^{\circ}\text{C}$ gave 0.216 g (56%) of pure **12** as a green crystalline solid. Anal. Calcd. (%) for $\text{C}_{12}\text{H}_{11}\text{Ti}$ (329.99): C 43.68; H 3.36. Found: C 43.06; H 3.74. ^1H NMR (200 MHz, C_6D_6 , 297 K) δ : 5.46 (s, 7H, C_7H_7), 5.03 (t, $J_{\text{H-H}} = 5.8$ Hz, 2H, C_5H_4), 4.68 (t, $J_{\text{H-H}} = 5.8$ Hz, 2H, C_5H_4). $^{13}\text{C}\{^1\text{H}\}$ NMR (50.3 MHz, C_6D_6 , 297 K) δ : 105.5 (s, C_5H_5), 99.7 (s, C_5H_4), 89.1 (s, C_7H_7).

2.11. Synthesis of $[(\eta^7\text{-C}_7\text{H}_7)\text{Ti}(\eta^5\text{-C}_5\text{H}_4\text{ZnCl})]$ (**13**)

A solution of ZnCl_2 (0.214 g, 1.57 mmol) in THF (12 mL) was added dropwise to a suspension of **1b** (0.548 g, 1.43 mmol) in hexane (10 mL) at $-78\text{ }^{\circ}\text{C}$. The reaction mixture was slowly warmed up to room temperature, and stirring was continued for 2 h. The color of the suspension turned from dark green to light green. The solid was filtered off and washed thoroughly with hexane. Drying *in vacuo* afforded 0.326 g (75%) of a light green powder. This was used directly for the next reaction without further purification and characterization.

2.12. Synthesis and characterization of $[(\eta^7\text{-C}_7\text{H}_7)\text{Ti}(\eta^5\text{-C}_5\text{H}_4)]_2$ (**14**)

A mixture of **12** (0.140 g, 0.435 mmol), **13** (0.165 g, 0.544 mmol) and $[\text{Pd}(\text{dppf})\text{Cl}_2]$ (5 mol%) in THF (15 mL) was heated at $60\text{ }^{\circ}\text{C}$ for 16 h. The solution was then concentrated to half of its volume, filtered and kept at $-30\text{ }^{\circ}\text{C}$ for 2 h. A green precipitate of **14** was isolated by filtration, washed with diethyl ether and dried *in vacuo*, yield: 0.045 g (25.5%). Anal. Calcd. (%) for $\text{C}_{24}\text{H}_{22}\text{Ti}_2$ (406.17): C 70.97; H 5.46. Found: C 64.90; H 5.15. ^1H NMR (200 MHz, C_6D_6 , 297 K) δ : 5.34 (s, 14H, C_7H_7), 5.02 (t, $J_{\text{H-H}} = 5.8$ Hz, 4H, C_5H_4), 4.87 (t, $J_{\text{H-H}} = 5.8$ Hz, 4H, C_5H_4). $^{13}\text{C}\{^1\text{H}\}$ NMR (50.3 MHz, C_6D_6 , 297 K) δ : 113.0 (s, *i*- C_5H_5), 96.8 (s, C_5H_4), 94.2 (s, C_5H_4), 87.8 (s, C_7H_7). MS (EI, 70 eV): m/z 406 (M^+). HR-MS (EI; m/z): Calcd for $\text{C}_{24}\text{H}_{22}\text{Ti}_2$ (M^+), 406.06808; found, 406.06827. UV/vis (toluene): λ_{max} (ϵ) = 686 (30).

2.13. Synthesis and characterization of $[(\eta^7\text{-C}_7\text{H}_7)\text{Ti}(\eta^5\text{-C}_5\text{H}_4\text{Ph})]$ (**15**)

A mixture of iodobenzene (0.085 g, 0.414 mmol), **13** (0.090 g, 0.296 mmol) and $[\text{Pd}(\text{dppf})\text{Cl}_2]$ (5 mol%) in THF (18 mL) was heated at $60\text{ }^{\circ}\text{C}$ for 16 h. After evaporation of the solvent, the residue was extracted with cold toluene and filtered through glass wool. Drying the filtrate under vacuum afforded a light green solid. Recrystallization from toluene at $-30\text{ }^{\circ}\text{C}$ gave 0.038 mg (46%) of pure **15** as a green crystalline solid. Anal. Calcd. (%) for $\text{C}_{18}\text{H}_{16}\text{Ti}$ (280.19): C 77.16; H 5.75. Found: C 76.05; H 5.89. ^1H NMR (200 MHz, C_6D_6 , 297 K) δ : 7.29–7.00 (m, 5H, C_5H_4), 5.38 (t, $J_{\text{H-H}} = 5.8$ Hz, 2H, C_5H_4), 5.34 (s, 7H, C_7H_7), 4.98 (t, $J_{\text{H-H}} = 5.8$ Hz, 2H, C_5H_4). $^{13}\text{C}\{^1\text{H}\}$ NMR (50.3 MHz, C_6D_6 , 297 K) δ : 143.5 (s, *i*- C_6H_5), 129.2 (s, C_6H_5), 127.1 (s, C_6H_5), 125.5 (s, C_6H_5), 98.6 (s, C_5H_5), 95.8 (s, C_5H_4), 88.5 (s, C_7H_7), 88.3 (s, *i*- C_5H_4). MS (EI, 70 eV): m/z 280 (M^+). HR-MS (EI; m/z): Calcd for $\text{C}_{18}\text{H}_{16}\text{Ti}$ (M^+), 278.07728; found, 278.07693.

2.14. Single-crystal X-ray structure determinations

Numerical details are summarized in Tables 1 and 2. Crystals were mounted in inert oil on glass fibers. Intensity measurements were performed at low temperature on Oxford Diffraction diffractometers using monochromated Mo $K\alpha$ or mirror-focused Cu $K\alpha$ radiation. Absorption corrections were based on multi-scans. Structures were refined anisotropically on F^2 using the program SHELXL-97 [30]. In several cases, the ring H atoms were refined freely or with distance restraints (see supplementary crystallographic data for details); other hydrogen atoms were included using idealized rigid methyl groups or a riding model. *Exceptions and special features*: Compounds **2** and **15** crystallize by chance in Sohncke space groups. Compound **8** displays a difference peak of $3.2\text{ e } \text{\AA}^{-3}$ close to the Ti atom. For compound **9**-THF, the THF was badly disordered and could not be refined satisfactorily; the program SQUEEZE [31] was therefore used to remove mathematically the effects of the solvent. The ethyl group of compound **11** is disordered. Several C atoms of compound **15** displayed irregular displacement ellipsoids, which were therefore constrained to be more regular using the program commands DELU and ISOR.

Table 1
Crystal and structure refinement data for **2**–**8**.

	2	3	4	5	6	7	8
Empirical formula	$\text{C}_{24}\text{H}_{21}\text{ClSiTi}$	$\text{C}_{20}\text{H}_{29}\text{ClSnTi}$	$\text{C}_{40}\text{H}_{58}\text{OSn}_2\text{Ti}_2$	$\text{C}_{30}\text{H}_{27}\text{PTi}_2$	$\text{C}_{30}\text{H}_{40}\text{BNSi}_2\text{Ti}_2$	$\text{C}_{34}\text{H}_{32}\text{Ti}_3$	$\text{C}_{32}\text{H}_{41}\text{ClTiZr}$
<i>a</i> (Å)	8.1585(2)	17.8885(4)	10.3880(6)	10.3366(2)	19.3186(6)	39.2431(14)	10.3369(2)
<i>b</i> (Å)	8.6708(2)	8.1679(2)	13.0499(6)	9.6075(2)	10.0599(2)	17.2466(8)	14.9335(2)
<i>c</i> (Å)	28.1704(6)	14.3083(2)	15.5167(6)	23.9270(2)	15.2774(6)	7.6738(2)	17.9112(2)
α ($^{\circ}$)	90	90	101.228(4)	90	90	90	90
β ($^{\circ}$)	90	101.086(2)	94.871(4)	94.814(2)	105.198(4)	90	99.783(2)
γ ($^{\circ}$)	90	90	107.948(4)	90	90	90	90
<i>V</i> (Å ³)	1992.79(8)	2051.60(7)	1939.00(16)	2367.78(7)	2865.22(15)	5193.7(3)	2724.68(7)
<i>Z</i>	4	4	2	4	4	8	4
Formula weight	420.85	471.47	888.04	514.29	577.42	584.30	600.22
Space group	$P2_12_12_1$	$P2_1/c$	$P\bar{1}$	$P2_1/n$	$C2/c$	$Fdd2$	$P2_1/c$
<i>T</i> (K)	100(2)	100(2)	100(2)	100(2)	100(2)	100(2)	100(2)
λ (Å)	1.54184	1.54184	1.54184	1.54184	0.17073	0.71073	1.54184
D_{calcd} (g cm ⁻³)	1.403	1.526	1.521	1.443	1.339	1.494	1.463
μ (mm ⁻¹)	5.476	14.146	13.712	6.486	0.661	0.923	6.657
Reflection collected	26,266	34,535	30,906	31,214	58,056	41,908	38,792
Independent reflections	4071 $R_{\text{int}} = 0.0376$	4245 $R_{\text{int}} = 0.0379$	7979 $R_{\text{int}} = 0.0208$	4890 $R_{\text{int}} = 0.0247$	3847 $R_{\text{int}} = 0.0605$	3088 $R_{\text{int}} = 0.0691$	5660 $R_{\text{int}} = 0.0270$
Goodness of fit on F^2	1.052	1.030	1.062	1.100	0.860	0.882	1.078
$R(F_o)$, [$I > 2\sigma(I)$]	0.0234	0.0188	0.0179	0.0248	0.0268	0.0309	0.0444
$R_w(F_o^2)$	0.0597	0.0512	0.0459	0.0698	0.0571	0.0543	0.1137
Flack parameter	0.000(5)	–	–	–	–	–0.02(2)	–
$\Delta\rho$ [e Å ⁻³]	0.257/–0.245	0.775/–0.577	0.523/–0.732	0.317/–0.406	0.354/–0.268	0.378/–0.221	3.248/–1.935

Table 2
Crystal and structure refinement data for **9**, **9**·THF, **10**–**12**, **14**, and **15**.

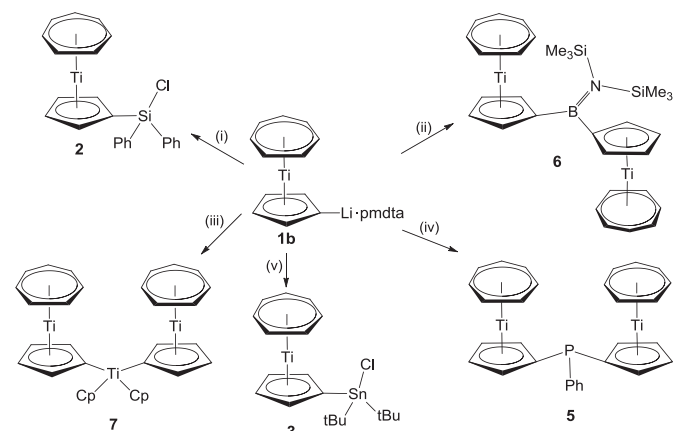
	9	9 ·THF	10	11	12	14	15
Empirical formula	C ₄₄ H ₄₂ O ₂ Ti ₂ Zr ₂	C ₄₈ H ₅₀ O ₂ Ti ₂ Zr ₂	C ₄₄ H ₄₂ O ₂ Ti ₂ Hf ₂	C ₂₄ H ₂₆ HfOTi	C ₁₂ H ₁₁ ITi	C ₂₄ H ₂₂ Ti ₂	C ₁₈ H ₁₆ Ti
<i>a</i> (Å)	10.1506(2)	44.4138(18)	10.1408(2)	15.7895(4)	12.5493(2)	10.4597(8)	10.828(2)
<i>b</i> (Å)	10.9013(2)	8.3540(2)	10.8733(2)	7.6609(2)	7.9906(2)	8.1360(6)	7.8912(16)
<i>c</i> (Å)	16.2339(4)	25.3490(10)	16.2218(2)	17.1629(6)	10.7922(2)	10.7751(13)	15.797(5)
α (°)	90	90	90	90	90	90	90
β (°)	104.544(2)	123.881(6)	104.731(2)	104.559(2)	93.750(2)	102.903(8)	97.91(3)
γ (°)	90	90	90	90	90	90	90
<i>V</i> (Å ³)	1738.79(6)	7808.3(5)	1729.89(5)	2009.39(10)	1079.89(4)	893.81(13)	1336.9(5)
<i>Z</i>	2	8	2	4	4	2	4
Formula weight	865.02	937.12	1039.56	556.84	330.01	406.22	280.21
Space group	<i>P</i> 2 ₁ / <i>c</i>	<i>C</i> 2/ <i>c</i>	<i>P</i> 2 ₁ / <i>c</i>	<i>P</i> 2 ₁ / <i>n</i>	<i>P</i> 2 ₁ / <i>c</i>	<i>P</i> 2 ₁ / <i>n</i>	<i>P</i> 2 ₁
<i>T</i> (K)	100(2)	100(2)	100(2)	100(2)	100(2)	100(2)	100(2)
λ (Å)	1.54184	1.54184	1.54184	0.71073	0.71073	1.54184	0.71073
<i>D</i> _{calcd} (g cm ⁻³)	1.652	1.594	1.996	0.848	1.036	1.509	1.392
μ (mm ⁻¹)	8.821	7.926	14.809	5.571	3.606	7.602	0.621
Reflection collected	17,238	46,302	20,351	49,844	30,198	11,482	47,404
Independent reflections	3614 <i>R</i> _{int} = 0.0287	8092 <i>R</i> _{int} = 0.0403	3571 <i>R</i> _{int} = 0.0267	5414 <i>R</i> _{int} = 0.059	2370 <i>R</i> _{int} = 0.0349	1842 <i>R</i> _{int} = 0.0952	5462 <i>R</i> _{int} = 0.1163
Goodness of fit on <i>F</i> ²	1.045	1.070	1.060	0.878	1.006	1.023	0.834
<i>R</i> (<i>F</i> _o), [<i>I</i> > 2 σ (<i>I</i>)]	0.0259	0.0262	0.0180	0.0206	0.0144	0.0527	0.0523
<i>R</i> _w (<i>F</i> _o ²)	0.0692	0.0710	0.0465	0.0259	0.0332	0.1443	0.1133
Flack parameter	—	—	—	—	—	—	−0.03(4)
$\Delta\rho$ [e Å ⁻³]	0.796/−0.707	0.537/−0.565	0.714/−0.843	1.101/−1.083	0.336/−0.354	0.750/−0.558	1.584/−0.736

3. Results and discussion

3.1. Synthesis and spectroscopic characterization of Cp-functionalized mono- and bitroticenes

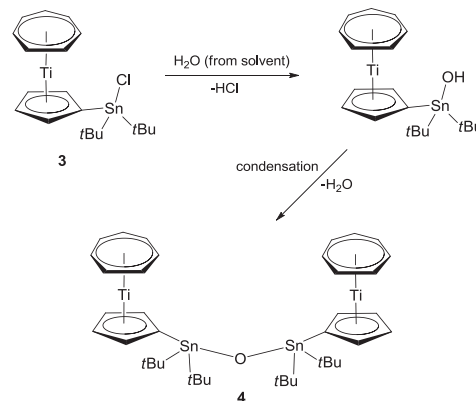
The monolithiated trocticene derivative [(η^7 -C₇H₇)Ti(η^5 -C₅H₄Li)]·pmdta (**1b**) was synthesized according to the published procedure [25]. Its treatment with stoichiometric amounts of dichlorodiphenylsilane (Ph₂SiCl₂) or dichlorodi-*tert*-butylstannane (tBu₂SnCl₂) in hexane at −78 °C afforded the trocticenyl chlorosilane **2** and the trocticenyl chlorostannane **3** as blue and blue-green crystalline solids in 78% and 42% yield, respectively. Similarly, **1b** reacted with half an equivalent of PhPCl₂, (Me₃Si)₂NBCl₂ and [(η^5 -C₅H₅)₂TiCl₂] to yield the phosphane-, borane- and titanocene-bridged bitroticenes **5**–**7** in almost quantitative yields (Scheme 1). Compound **3** partially hydrolyzed in the presence of moisture, and presumably, the condensation of an intermediate organotin hydroxide resulted in the formation of the bis(trocticenyl) organostannoxane **4** as a green solid (Scheme 2).

The bimetallic trocticenyl–zirconium complex **8** was obtained as a by-product in very low yield during our attempts to synthesize

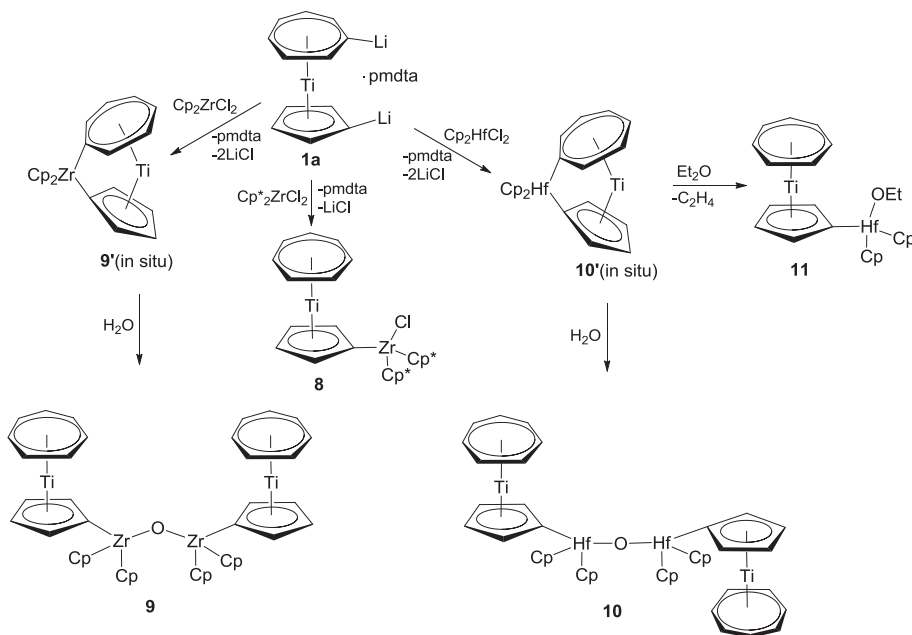


Scheme 1. Synthesis of Cp-substituted trocticenes; reagents: (i) Ph₂SiCl₂; (ii) 0.5 eq. Cl₂BN(SiMe₃)₂; (iii) 0.5 eq. [Cp₂TiCl₂]; (iv) 0.5 eq. PhPCl₂; (v) tBu₂SnCl₂.

a zircona[1]trocticenophane by the reaction of the dilithiated trocticene [(η^7 -C₇H₆Li)Ti(η^5 -C₅H₄Li)]·pmdta (**1a**) [25] with 1 eq. of [(η^5 -C₅Me₅)₂ZrCl₂]. Similar reactions with the sterically less hindered zirconocene and hafnocene dichlorides, [(η^5 -C₅H₅)₂ZrCl₂] and [(η^5 -C₅H₅)₂HfCl₂], also failed to furnish the desired Zr- or Hf-bridged *ansa*-Cht-Cp complexes **9'** and **10'** (Scheme 3), and the μ -oxo zirconocene- and hafnocene-bridged bitroticenes **9** and **10** were the only compounds that could be isolated from hexane solutions. In view of similar reactivities reported for zircona- and hafna[1]ferrocenophanes upon exposure to moist air [32], we assume that the formation of **9** and **10** can also be ascribed to the reaction of **9'** and **10'** with residual water from the solvent or the glassware. Unfortunately, all attempts to isolate these strained complexes under strictly inert conditions proved unsuccessful and always afforded the μ -oxo species **9** and **10**. This observation is in contrast to the recent report by Braunschweig et al. on the isolation of a [1]trochrocenophane containing a bridging [(η^5 -C₅H₄tBu)₂Zr] moiety [24]. Our failure to isolate **9'** and **10'** might be ascribed to insufficient steric protection of the *ipso*-C₇H₆–metal bonds by the C₅H₅ ligands and also to higher strain, since the titanium–carbon bonds in trocticenes are longer than the chromium–carbon bonds in



Scheme 2. Hydrolysis of compound **3** and formation of the organostannoxane **4**.

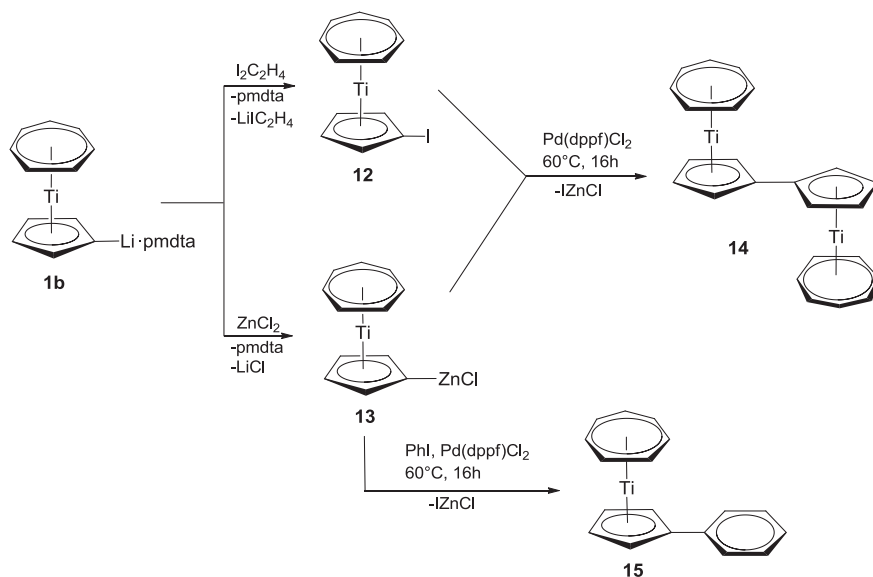


Scheme 3. Attempted synthesis of Zr- and Hf-bridged [1]trocenophanes.

trocenophanes [18,19]. Further evidence for the high reactivity of **10'** stems from an attempted recrystallization of the reaction mixture from diethyl ether, which afforded crystals of the ethoxide complex **11**; this might have formed by ether cleavage and elimination of ethylene promoted by **10'** (Scheme 3).

The reactions of **1b** with 1,2-diiodoethane and zinc dichloride (ZnCl_2) furnished the iodo- and zinc-substituted trocencenes **12** and **13** as green solids in good yield. Negishi carbon–carbon cross-coupling between both compounds catalyzed by $[\text{Pd}(\text{dppf})\text{Cl}_2]$ afforded the interannularly bridged [5–5]bitrocenene **14** as a green crystalline solid in 26% yield. Similarly, the phenyl-substituted trocencene **15** was obtained in 46% yield through a coupling reaction between **13** and iodobenzene (Scheme 4).

Compounds **2–7**, **12**, **14** and **15** are readily soluble in nonpolar solvents such as hexane and/or toluene, while compounds **8–11** are sparingly soluble in hexane but readily dissolve in tetrahydrofuran and dichloromethane. All compounds are sensitive toward air and moisture but can be stored in a glove box in an argon atmosphere for several months. Except for compounds **4** and **11**, which could not be isolated in sufficient quantities for NMR spectroscopic characterization, the ^1H NMR spectra of all complexes showed a splitting pattern characteristic for substituted Cp rings, whereby two pseudotriplet resonances assigned to the α - and β - C_5H_4 protons are observed in the range from 4.62 (**12**) to 5.58 ppm (**8**); the C_7H_7 protons give rise to a singlet resonance between 5.34 (**14**, **15**) and 5.83 ppm (**9**). In addition, the ^1H NMR spectrum of the



Scheme 4. Negishi cross-coupling reactions involving the zincated trocencene **13**.

troticenylic chlorostannane **3** exhibits long-range $^3J(^1\text{H}-^{117/119}\text{Sn})$ and $^4J(^1\text{H}-^{117/119}\text{Sn})$ coupling constants of 12.8/17.9 and 12.3/17.3 Hz, respectively, between the tin atom and the Cp hydrogen atoms. The resonance for the *tert*-butyl protons appears at 1.24 ppm and shows $^2J(^1\text{H}-^{117/119}\text{Sn})$ coupling constants of 82.9/86.7 Hz.

The ^{13}C NMR spectra of compounds **2**, **3**, **6**, **7**, **9**, **10** and **12** display three resonances for the Cp ring ranging from 100.0 (**3**) to 147.3 ppm (**9**). The magnetically equivalent Cht carbon atoms in the ^{13}C NMR spectra of **2**, **3**, **6**, **7**, **9**, **10** and **12** are observed as singlet resonances between 85.5 (**9**) and 89.1 ppm (**12**). These values are close to that reported for the C_7H_7 carbon NMR signal in troiticene (86.4 ppm) [26]. The ^{13}C NMR resonance for the quaternary *t*Bu carbon atoms in **3** is found at 36.0 ppm with $^1J(^{13}\text{C}-^{117/119}\text{Sn}) = 423.7/402.3$ Hz, which falls in the expected range for a four-coordinate tin atom [33]. The ^{119}Sn NMR spectrum of **3** showed a single resonance at 30.3 ppm, which is significantly shifted to higher field in comparison with the value reported for the ferrocene analogue $[(\eta^5\text{-C}_5\text{H}_5)\text{Fe}(\eta^5\text{-C}_5\text{H}_4\text{SnCl}t\text{Bu}_2)]$ ($\delta = 72.3$ ppm) [34]. As a result of coupling with the phosphorus atom, the Cp carbon atoms in the ^{13}C NMR spectrum of **5** appear as doublet resonances at 103.2 (*ipso*-C), 101.8 and 100.2 ppm with $^1J(^{13}\text{C}-^{31}\text{P})$, $^2J(^{13}\text{C}-^{31}\text{P})$ and $^3J(^{13}\text{C}-^{31}\text{P})$ coupling constants of 17.0, 9.8 and 2.8 Hz, respectively. The ^{31}P NMR spectrum of **5** shows a single resonance at -29.2 ppm, shifted to higher field in comparison with $[(\eta^7\text{-C}_7\text{H}_7)\text{Ti}(\eta^5\text{-C}_5\text{H}_4\text{PPh}_2)]$ ($\delta = -17.5$ ppm) [25,28]. The ^{11}B NMR spectrum of **6** displays a broad resonance at 36.7 ppm. The UV/vis spectrum of [5-5]bitroticene (**14**) was recorded in toluene, showing a weak band at 689 nm ($\epsilon = 30$ L mol $^{-1}$ cm $^{-1}$), which is similar to the values reported for troiticene [11a,16,35]. For **14** and **15**, the molecular ions $[(\eta^7\text{-C}_7\text{H}_7)\text{Ti}(\eta^5\text{-C}_5\text{H}_4\text{Ph})]^+$ and $[(\eta^7\text{-C}_7\text{H}_7)\text{Ti}(\eta^5\text{-C}_5\text{H}_4)]^+$ were detected at $m/z = 280$ and 406 by electron ionization mass spectrometry (EI-MS).

3.2. Molecular structures of the Cp-functionalized monotroticenes **2**, **3**, **8**, **11**, **12** and **15**

Suitable crystals for X-ray structure determinations were obtained by cooling saturated solutions of the compounds in pentane (**3**), toluene (**2**, **12**, **15**) and Et $_2$ O (**11**) at -30 °C or by slow evaporation of a THF/hexane solution of **8** at room temperature. The molecule of compound **12** displays approximate mirror symmetry (r.m.s. deviation 0.24 Å). Compound **15** crystallizes with two independent but similar molecules differing only in the orientation of the phenyl ring (a least-squares fit gave an r.m.s. deviation of 0.09 Å); only one is discussed here. The molecular structures of all these compounds are shown in Figs. 3–8, and selected bond lengths and angles are summarized in Table 3.

The bond distances between the titanium atom and the carbon atoms of the five-membered rings fall in the ranges 2.3273(17)–2.3411(17) (**2**), 2.3226(16)–2.3345(17) (**3**), 2.284(4)–2.395(3) (**8**), 2.305(2)–2.339(2) (**11**), 2.3236(17)–2.3469(17) (**12**) and 2.315(5)–2.349(5) (**15**) Å. As expected, and in agreement with the molecular structure of the unsubstituted troiticene [36], the Ti–C $_5\text{H}_4$ carbon bonds are significantly longer than the corresponding Ti–C $_7\text{H}_7$ distances [2.2020(19)–2.2122(18) (**2**), 2.1996(17)–2.2221(18) (**3**), 2.209(4)–2.253(5) (**8**), 2.201(3)–2.223(3) (**11**), 2.1944(17)–2.2106(17) (**12**), 2.198(6)–2.212(5) (**15**) Å], reflecting the stronger metal–ligand interactions with the Cht ring [19]. The two rings are nearly parallel, as evidenced by the Cp $_{\text{ct}}$ –Ti–Cht $_{\text{ct}}$ (ct = ring centroid) angles of 177.9° (**2**), 174.3° (**3**), 170.1° (**8**), 174.2° (**11**), 177.2° (**12**) and 178.0° (**15**) (Table 1). These values deviate only slightly from the ideal linear arrangement, with the maximum deviation being observed for the zirconocene-bridged troiticene **8**. The silicon and tin atoms in compounds **2** and **3** adopt distorted tetrahedral configurations with the angles about the Si and Sn

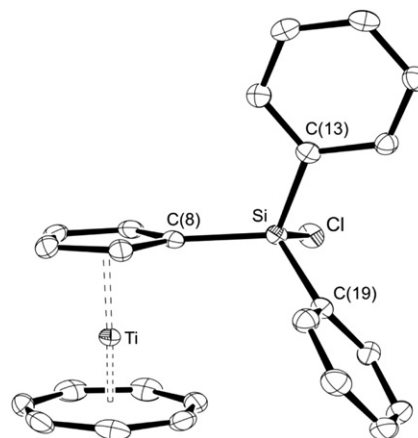


Fig. 3. ORTEP diagram of **2** with thermal displacement parameters drawn at the 50% probability level. Selected bond lengths [Å] and angles [°]: Si–Cl = 2.0694(6), Si–C(13) = 1.8603(17), Si–C(19) = 1.8599(17), C(8)–Si–Cl = 106.5(6), C(8)–Si–C(19) = 113.9(8), C(8)–Si–C(13) = 110.8(8), C(19)–Si–C(13) = 109.1(7), C(19)–Si–Cl = 108.3(6), C(13)–Si–Cl = 108.2(5).

atoms ranging from 106.5(8)° to 113.9(8)° and from 100.5(5)° to 118.1(7)°. The Si–C(8) distance of 1.8540(17) Å in **2** is similar to the Si–C(phenyl) bond lengths of 1.8599(17) and 1.8603(17) Å, while the Sn–C(8) distance of 2.1218(16) Å in **3** is slightly shorter than the two Sn–C(*t*Bu) bonds of 2.1743(17) and 2.1828(17) Å. The Si–Cl and Sn–Cl bonds of 2.0694(6) and 2.3915(4) Å are close to those reported for related ferrocenyl chlorosilanes and chlorostannanes; e.g. 2.0802(10) Å in $[(\eta^5\text{-C}_5\text{H}_5)\text{Fe}(\eta^5\text{-C}_5\text{H}_4)]_3\text{SiCl}$ [37a], 2.080(1) Å in $[(\eta^5\text{-C}_5\text{H}_4\text{SiClPh}_2)\text{Fe}(\eta^5\text{-C}_5\text{H}_4)]_2\text{BCl}$ [37b], and 2.4026(26) Å in $[(\eta^5\text{-C}_5\text{H}_5)\text{Fe}(\eta^5\text{-C}_5\text{H}_3\text{SnClMe}_2)(\text{BClPh})]$ [38].

The C(8)–I distance of 2.0797(17) Å in **12** and the C(8)–C(13) distance of 1.467(8) Å in **15** are in agreement with the corresponding bond lengths reported for the ferrocenyl iodide $[(\eta^5\text{-C}_5\text{H}_5)\text{Fe}(\eta^5\text{-C}_5\text{H}_3\text{I})(\text{CHO})]$ [2.083(7) Å] [39] and for the phenyltroiticene $[(\eta^5\text{-C}_7\text{H}_7)\text{V}(\eta^5\text{-C}_5\text{H}_4\text{Ph})]$ [1.478(15) Å] [40]. The interplanar angle between the C $_5\text{H}_4$ ring and the phenyl substituent in **15** is 17.9(2)°. The zirconium and hafnium atoms in compounds **8** and **11** adopt a characteristic, strongly distorted pseudo-tetrahedral configuration with the Cp $_{\text{ct}}$ –Zr–Cht $_{\text{ct}}$ and Cp $_{\text{ct}}$ –Hf–Cht $_{\text{ct}}$ angles of 134.6° (**8**) and 129.5° (**11**) and the C(8)–Zr–Cl and C(8)–Hf–O angles of 91.5(9)° (**8**) and 98.7(8)° (**11**), respectively. Thereby, the

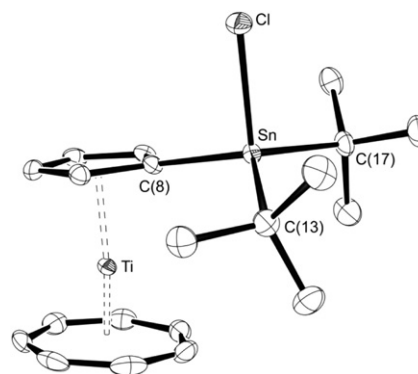


Fig. 4. ORTEP diagram of **3** with thermal displacement parameters drawn at the 50% probability level. Selected bond lengths [Å] and angles [°]: Sn–Cl = 2.3915(4), Sn–C(13) = 2.1743(17), Sn–C(17) = 2.1828(17), C(8)–Sn–Cl = 100.5(5), C(8)–Sn–C(17) = 117.1(6), C(8)–Sn–C(13) = 113.4(7), C(17)–Sn–C(13) = 118.1(7), C(17)–Sn–Cl = 101.2(5), C(13)–Sn–Cl = 102.4(5).

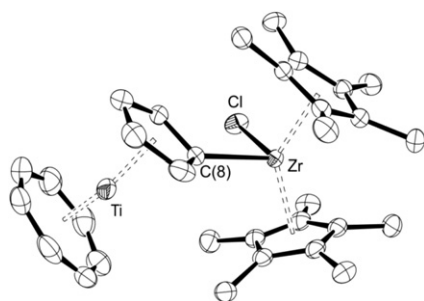


Fig. 5. ORTEP diagram of **8** with thermal displacement parameters drawn at the 50% probability level. Selected bond lengths [Å] and angles [°]: Zr–Cl = 2.4425(9), Zr–C_{cp} = 2.523(3)–2.604(3), C(8)–Zr–Cl = 91.5(9), C(8)–Zr–C_{cp} = 103.0 and 111.5, C_{cp}–Zr–Cl = 103.1 and 104.7, C_{cp}–Zr–C_{cp} = 134.6.

angles at Zr in **8** are very similar to those in the closely related ferrocenyl-zirconium derivative [(η⁵-C₅H₅)Fe{η⁵-C₅H₄ZrCl(η⁵-C₅Me₅)₂}] [135.4(1)° and 91.9(1)°], which also exhibits almost identical [Zr–Cl = 2.456(2) Å, Zr–C = 2.314(7) Å] distances to those in **8** (Table 3) [41].

3.3. Molecular structures of the Cp-functionalized bitroticenes **4–7**, **9**, **9**·THF, **10** and **14**

Single crystals for X-ray diffraction analysis were obtained by cooling saturated solutions of the compounds in toluene (**5**, **7**, **9**, **10**) or diethyl ether (**14**) or by slow evaporation of a solution of the respective compound in THF (**9**·THF), hexane (**4**) and THF/diethyl ether (1:2) (**6**) at room temperature. Compound **9** crystallized without solvent from toluene solution, but as **9**·THF from tetrahydrofuran solution. The molecular structures of complexes **4–7**, **9**·THF, **10** and **14** are presented in Figs. 9–15. Selected bond distances and angles are assembled in Table 4. The molecular structures of **9** and **10** are isotopic, and therefore, only the structure of **10** is shown (Fig. 14).

In a similar fashion to that discussed for the monotroticenes (*vide supra*), all Cht–Cp sandwich moieties are affected by the variable substitution pattern, and the maximum deviation from an ideal C_{cp}–Ti–Cht_{ct} angle of 180° is observed for **7** (170.5° for both troiticenyl fragments). Similar Ti–C bond lengths are also observed, with the metal–carbon distances to the seven-membered ring being significantly shorter than those to the five-membered ring

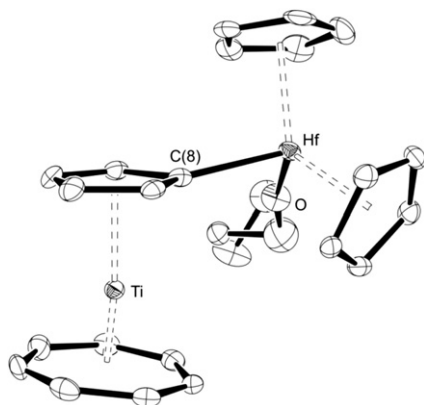


Fig. 6. ORTEP diagram of **11** with thermal displacement parameters drawn at the 50% probability level. The carbon atoms of the ethanoate fragment are disordered over two positions. Selected bond lengths [Å] and angles [°]: Hf–O = 1.9075(17), Hf–C_{cp} = 2.502(3)–2.541(3), C(8)–Hf–O = 98.6(8), C(8)–Hf–C_{cp} = 101.7/106.7, C_{cp}–Hf–O = 107.9 and 108.0, C_{cp}–Hf–C_{cp} = 129.5.

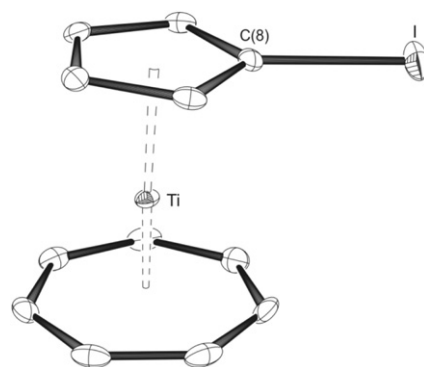


Fig. 7. ORTEP diagram of **12** with thermal displacement parameters drawn at the 50% probability level.

(Table 4). Compound **4** represents, to the best of our knowledge, the first example of a structurally characterized metallocene-supported organostannoxane in which the tin atoms are directly bound to the C_nH_{n-1} ring. In contrast, organostannoxanes containing ferrocene units have been obtained from the reaction between ferrocenyl carboxylic acid and an organotin oxide or hydroxide, leading to C(O)O-bridged molecules [42,43]. Both tin atoms in **4** reside in a distorted tetrahedral environment with the angles ranging between 101.7(6)° and 114.9(7)° (at Sn1) and between 107.5(6)° and 120.0(7)° (at Sn2). The Sn(1)–C(8) and Sn(2)–C(20) distances are 2.1374(17) and 2.1491(16) Å, which is markedly longer than the corresponding distance in **3** [2.1218(16) Å] and the Sn(1)–C(15) bond length in the dimeric diferrocenyltin dihydroxide [(η⁵-C₅H₅)Fe{η⁵-C₅H₃(CH₂NMe₂)₂Sn(OH)₂}]₂ [2.12(2) Å] [44]. The bent nature of the stannoxane core is reflected by the Sn(1)–O–Sn(2) angle of 145.2(7)°, which is somewhat larger than the corresponding angle found in hexaphenyldistannoxane, (Ph₃Sn)₂O [137.8(3)°] [45], and deviates considerably from a linear arrangement as reported for the distannoxanes (tBu₃Sn)₂O [46] and [(PhCH₂)₃Sn]₂O [47].

The overall structure of the phosphorus-bridged bitroticene **5** is very similar to the corresponding biferoenylphenylphosphane [(η⁵-C₅H₅)Fe(η⁵-C₅H₄)₂PPh] [48] with the sandwich moieties adopting an almost perpendicular orientation, as indicated by an angle of 81.2(6)° between the two Cp planes. The boron-bridged complex **6** displays crystallographic C₂ symmetry, and substitution of the trigonal-pyramidal phosphorus atom in **5** by a trigonal-planar boron atom in **6** affords an *anti*-orientation of the troiticene moieties with Cp ligands that deviate by 26.1(6)° from a perfectly coplanar orientation. The angle between the NSi₂ and BC₂ planes is 72.4(3)°, indicating that an effective B–N π-interaction is not possible, and consequently, the B–N bond length [1.468(3) Å] in **6** is considerably longer than observed for the planar species

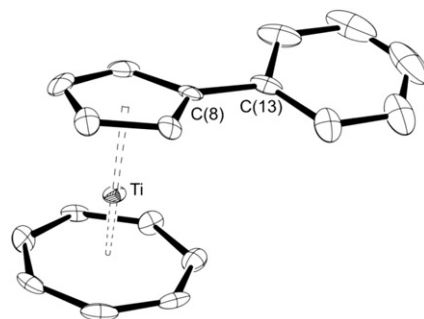


Fig. 8. ORTEP diagram of **15** with thermal displacement parameters drawn at the 50% probability level.

Table 3Selected bond lengths (Å) and angles in **2**, **3**, **8**, **11**, **12** and **15**.

	2	3	8	11	12	15
	E = Si	E = Sn	E = Zr	E = Hf	E = I	E = C(13)
Ti–C _{cht}	2.2020(19)–2.2122(18)	2.1996(17)–2.2221(18)	2.209(4)–2.253(5)	2.201(3)–2.223(3)	2.1944(17)–2.1940(17)	2.201(5)–2.214(5)
Ti–C _{cp}	2.3273(17)–2.3411(17)	2.3226(16)–2.3345(17)	2.284(4)–2.395(3)	2.305(2)–2.339(2)	2.3236(17)–2.3469(17)	2.313(5)–2.349(5)
Ti–C _{t7}	1.486	1.492	1.539	1.496	1.481	1.475
Ti–C _{t5}	1.998	1.994	1.966	1.980	2.002	1.992
E–C(8)	1.8540(17)	2.1218(16)	2.323(3)	2.275(2)	2.0797(17)	1.465(8)
C _{cp} –Ti(1)–C _{ht} _{ct}	177.9	174.3	170.1	174.2	177.2	178.0

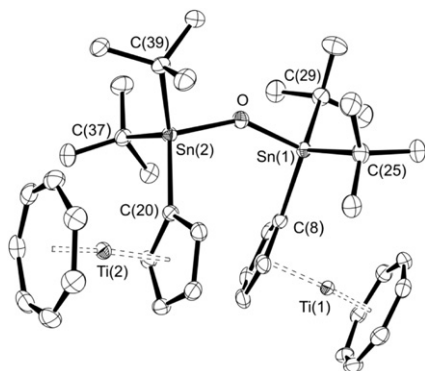


Fig. 9. ORTEP diagram of **4** with thermal displacement parameters drawn at the 50% probability level. Selected bond lengths [Å] and angles [°]: Sn(1)–O = 1.9569(12), Sn(2)–O = 1.9575(12), Sn(1)–C(25) = 2.1832(17), Sn(1)–C(29) = 2.1784(18), Sn(2)–C(33) = 2.1881(17), Sn(2)–C(37) = 2.1864(18), C(8)–Sn(1)–O = 104.5(6), C(8)–Sn(1)–C(25) = 114.9(7), C(8)–Sn(1)–C(29) = 113.8(7), C(25)–Sn(1)–C(29) = 115.7(7), C(25)–Sn(1)–O = 104.2(6), C(29)–Sn(1)–O = 101.7(6), C(20)–Sn(2)–O = 107.5(6), C(20)–Sn(2)–C(33) = 115.1(7), C(20)–Sn(2)–C(37) = 109.3(7), C(33)–Sn(2)–C(37) = 102.0(7), C(33)–Sn(2)–O = 97.9(6), C(37)–Sn(2)–O = 105.3(6), Sn(1)–O–Sn(2) = 145.2(7).

(C₆F₅)₂BN(CH₂)₄ [1.366(3)°] [49]. The titanocene-bridged complex **7** also displays crystallographic C₂ symmetry but is close to C_{2v} (r.m.s. deviation 0.11 Å), with a pseudo-tetrahedral geometry at the Ti(2) atom. Interestingly, **7** can be regarded as a dimetalated derivative of tetrakis(cyclopentadienyl) titanium, which was shown to exhibit fast hapticity interconversion in solution and to display a [(η⁵-C₅H₅)₂Ti(η¹-C₅H₅)₂] structure in the solid state [50,51]. Similar structural features to those found in **7** (Table 2) were also reported for Cp₂Ti-bridged biferrocenes such as [(η⁵-C₅H₅)Fe(η⁵-C₅H₄)₂][Ti(η⁵-C₅H₅)₂] [52] and [(η⁵-C₅H₄-CH₂N(CH₃)₂)Fe(η⁵-C₅H₄)₂][Ti(η⁵-C₅H₅)₂] [53].

The isotopic complexes **9** (solvent-free form) and **10** crystallize with imposed inversion symmetry (and approximate C_{2h} symmetry, r.m.s. deviation 0.12 Å), furnishing exactly linear

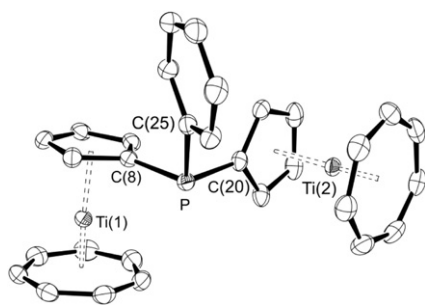


Fig. 10. ORTEP diagram of **5** with thermal displacement parameters drawn at the 50% probability level. Selected bond lengths [Å] and angles [°]: P–C(20) = 1.8232(14), P–C(25) = 1.8381(13), C(8)–P–C(20) = 98.3(6), C(8)–P–C(25) = 100.0(6), C(25)–P–C(20) = 102.3(6).

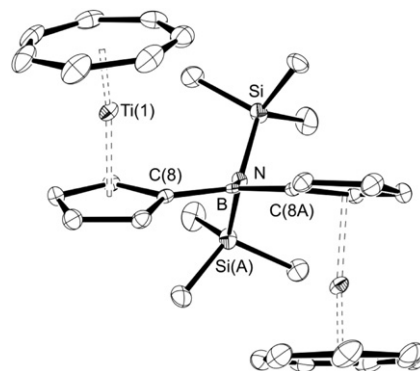


Fig. 11. ORTEP diagram of **6** with thermal displacement parameters drawn at the 50% probability level. Selected bond lengths [Å] and angles [°]: B–N = 1.468(3), N–Si = 1.7456(8), C(8)–B–C(8A) = 122.3(17), C(8)–B–N = 118.83(8), B–N–Si = 119.20(4).

Zr–O–Zr(A) and Hf–O–Hf(A) angles and short Zr–O and Hf–O bond lengths of 1.94560(14) and 1.9364(1) Å, whereas the formally C₁-symmetric molecule in **9**·THF (the approximate symmetry is twofold, r.m.s. deviation 0.11 Å) displays a bent Zr(1)–O–Zr(2) arrangement [165.5(8)°] with Zr–O bond lengths of 1.9427(13) and 1.9651(13) Å. Similar structural parameters were reported for the oxo-bridged dinuclear complexes [(Cp₂ZrMe)₂(μ-O)] [54] and [(Cp₂HfMe)₂(μ-O)] [55]. Finally, the pentafulvalene complex **14** adopts an exact *trans*-conformation with the cyclopentadienyl rings being perfectly coplanar, as a consequence of crystallographic inversion symmetry (and approximate C_{2h} symmetry, r.m.s. deviation 0.07 Å). Such an ideally parallel orientation of the trocicenyl units in **14** has been previously observed in the crystal structures of biferrocene, [(η⁵-C₅H₅)Fe(η⁵-C₅H₄)₂] [56], and [5–5]bitrovacene, [(η⁷-C₇H₇)V(η⁵-C₅H₄)₂] [40]. This is in contrast to the crystal structure of [7–7]bitrovacene [(η⁵-C₅H₅)V(η⁷-C₇H₆)₂], in which the trocicenyl fragments are almost perpendicular to one another [57]. In **14**, the Cp and Cht rings in each trocicenyl moiety are nearly coplanar as evidenced by the dihedral angle between both planes [1.42(1)°], which is smaller than the corresponding angle of 2.2(3)°

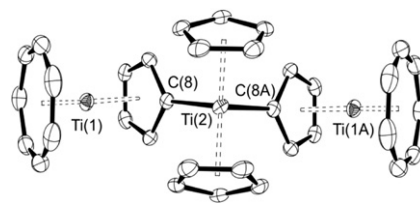


Fig. 12. ORTEP diagram of **7** with thermal displacement parameters drawn at the 50% probability level. Selected bond lengths [Å] and angles [°]: Ti(2)–C_{cp} = 2.394(2)–2.419(2), C(8)–Ti(2)–C(8A) = 92.0(11), C(8)–Ti(1)–C_{cp} = 106.0 and 107.7, C_{cp}–Ti(2)–C_{cp} = 130.8.

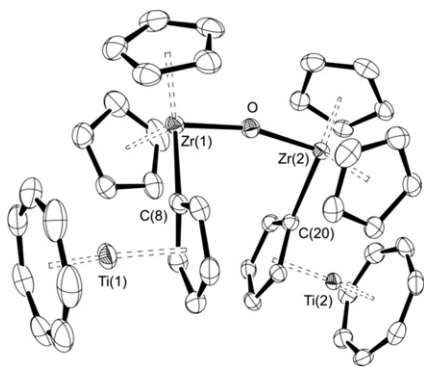


Fig. 13. ORTEP diagram of **9**-THF with thermal displacement parameters drawn at the 50% probability level. Selected bond lengths [Å] and angles [°]: Zr(1)–O = 1.9427(13), Zr(2)–O = 1.9651(13), Zr(1)–C_{cp} = 2.518(2)–2.569(2), Zr(2)–C_{cp} = 2.2927(18)–2.5701(19), C(8)–Zr(1)–O = 96.2(6), C(8)–Zr(1)–C_{cp} = 105.6/105.8, O–Zr(1)–C_{cp} = 106.7/108.4, C(20)–Zr(2)–O = 95.7(6), C(20)–Zr(2)–C_{cp} = 105.8/106.2, O–Zr(2)–C_{cp} = 106.4 and 107.8, C_{cp}–Zr(1)–C_{cp} = 129.3, C_{cp}–Zr(2)–C_{cp} = 128.8, Zr(1)–O–Zr(2) = 165.5(8).

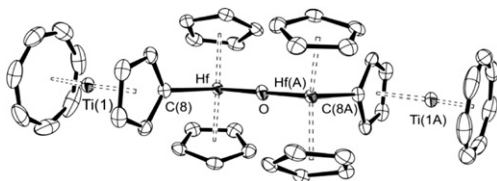


Fig. 14. ORTEP diagram of **10** with thermal displacement parameters drawn at the 50% probability level. Selected bond lengths [Å] and angles [°]: Hf–O = 1.9364(1), Hf–C_{cp} = 2.509(2)–2.543(2), C(8)–Hf–O = 90.8(6), C(8)–Hf–C_{cp} = 106.6 and 108.6, O–Hf–C_{cp} = 107.9 and 109.2, C_{cp}–Hf–C_{cp} = 127.5, Hf–O–Hf(A) = 180.0. Compound **9** is isotopic to **10**.

found in the non-bridged trocticene [(η⁷-C₇H₇)Ti(η⁵-C₅H₅)] [58]. The C–C bond lengths (Table 4) within the cyclopentadienyl ligand [1.417(6)–1.419(5) (mean 1.417) Å] in **14** are slightly lengthened as compared with those reported for trocticene [1.386(5)–1.404(8) (mean 1.396) Å] [58], but they are in agreement with those measured in biferrrocene [C–C = 1.35–1.45 (mean 1.40) Å] [56] and [5–5]bitrovacene [C–C = 1.406(2) Å (mean)] [40]. In these structures, the lengths of the C–C bond linking two Cp rings [1.48(4) Å and 1.468(5) Å, respectively] are close to the 1.464(7) Å found in **14**.

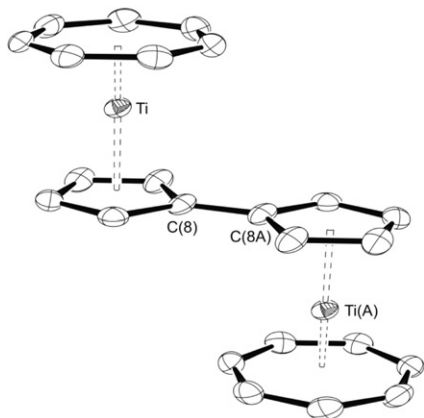


Fig. 15. ORTEP diagram of **14** with thermal displacement parameters drawn at the 50% probability level.

Table 4
Selected bond lengths (Å) and angles in **4–7**, **9**, **9**-THF, **10**, and **14**.

	4	5	6	7	9	9 -THF	10	14
Ti(1)–C _{ht}	2.2087(18)–2.2269(19)	2.1940(15)–2.2232(14)	2.2053(16)–2.2190(15)	2.198(2)–2.235(3)	2.193(3)–2.216(3)	2.198(3)–2.236(2)	2.193(3)–2.216(3)	2.199(4)–2.217(4)
Ti(2)–C _{ht}	2.1975(19)–2.2292(19)	2.1967(14)–2.2103(15)	2.3207(13)–2.3373(14)	2.310(2)–2.349(2)	2.303(2)–2.355(2)	2.208(2)–2.235(2)	2.303(2)–2.355(2)	2.317(4)–2.344(3)
Ti(1)–C _{cp}	2.3163(17)–2.3441(18)	2.3175(14)–2.3431(13)	2.3120(13)–2.3382(14)	2.310(2)–2.349(2)	2.303(2)–2.355(2)	2.2969(19)–2.341(2)	2.303(2)–2.355(2)	2.317(4)–2.344(3)
Ti(2)–C _{cp}	2.3167(17)–2.3435(18)	2.3120(13)–2.3382(14)	2.3120(13)–2.3382(14)	2.310(2)–2.349(2)	2.303(2)–2.355(2)	2.3008(19)–2.3425(19)	2.303(2)–2.355(2)	2.317(4)–2.344(3)
Ti(1)–C _{T7}	1.497	1.486	1.494	1.503	1.527	1.503	1.502	1.486
Ti(2)–C _{T7}	1.497	1.480	1.493	1.985	1.983	1.501	1.986	1.990
Ti(1)–C _{T5}	1.993	1.991	1.993	1.985	1.983	1.978	1.986	1.990
Ti(2)–C _{T5}	1.994	1.991	1.993	2.419(2)	2.2919(19)	1.982	2.264(2)	1.464(7)
E(1)–C(8)	2.1374(17)	1.8320(13)	1.5585(16)		2.2919(19)	2.2943(19)	2.264(2)	
E(2)–C(20)	2.1491(16)	1.8232(14)			1.9456(14)	2.2927(18)	1.9364	
E(1)–O					1.9456(14)	1.9427(13)	1.9364	
E(2)–O					169.9	1.9651(13)	174.71	
C _{cp} –Ti(1)–C _{ht}	175.3	176.1	173.7	170.51	169.9	172.6	174.71	179.2
C _{cp} –Ti(2)–C _{ht}	174.7	177.7				173.2		

4. Conclusion

A series of Cp-substituted trocticene and bitrocticene complexes have been synthesized and characterized starting from mono- or dilithiated trocticene. These compounds represent important examples for the direct attachment of different substituents to the Cp ring including halide, chloroorganosilane, chloroorganostannane or metallocene monochloride. The presence of functional bonds such as C₅H₄–I, C₅H₄–Si–Cl, C₅H₄–Sn–Cl or C₅H₄–Zr–Cl in these complexes allows their use as synthons for further reactions. Indeed, the trocticenyl chloroorganostannane **3** is partially converted to the organostannoxane **4** when exposed to moisture. Compound **4** represents the first structurally characterized metallocene-supported organostannoxane with a direct C₅H₄–Sn bond. Using the trocticenyl iodide **12** and iodobenzene, we also achieved successful palladium-catalyzed Negishi C–C cross-coupling reactions and isolated the fulvalene complexes **14** and **15**. Further important findings described in this work are the heterobimetallic oxo complexes **9** and **10** isolated during our attempts to obtain the zircona- and hafna[1]trocticenophanes **9'** and **10'**. These latter might exist in solution, but appear to undergo a rapid and regioselective (at the seven-membered ring) *ipso*-C–M bond cleavage in contact with any trace of moisture from the solvent or the glassware. The attempt to incorporate Cp₂*Zr [Cp* = (η⁵-C₅Me₅)] in order to protect the *ipso*-C–M bond and reduce this high reactivity observed in **9'** and **10'** was unsuccessful. Only a monosubstitution reaction occurred (compound **8**), probably due to the steric hindrance at the Cp*Zr fragment. Consequently, further investigations will focus on the use of an appropriate ligand, Cp₂'M [M = Zr, Hf; Cp' = (η⁵-C₅H₄tBu)], which has the advantage of being more sterically hindered than Cp but significantly less than Cp*, and which has been successfully introduced into the *ansa*-bridge of [1]ferro- and [1]trochrocenophanes [24,32].

Acknowledgments

This work was partially supported by the Deutsche Forschungsgemeinschaft through the focus program SPP 1118 “Secondary Interactions as a Steering Principle for the Selective Functionalization of Non-Reactive Substrates” [59]. A.C.T.K is grateful to the Alexander von Humboldt Foundation for a post-doctoral fellowship.

Appendix A. Supplementary material

CCDC 839987–840000 contain the supplementary crystallographic data for this paper. These data can be obtained free of charge from The Cambridge Crystallographic Data Centre via www.ccdc.cam.ac.uk/data_request/cif.

References

- [1] G. Wilkinson, M. Rosenblum, M.C. Whiting, R.B. Woodward, *J. Am. Chem. Soc.* **74** (1952) 2125.
- [2] E.O. Fischer, W. Pfab, *Z. Naturforsch.* **7b** (1952) 377.
- [3] Special issue: 50th anniversary of the discovery of ferrocene. in: R.D. Adams (Ed.), *J. Organomet. Chem.* (2001), pp. 637–639.
- [4] B. Bildstein, *Coord. Chem. Rev.* **206–207** (2000) 369.
- [5] (a) T.J. Colacot, *Platinum Met. Rev.* **45** (2001) 22; (b) R.G. Arrayás, J. Adrio, J.C. Carretero, *Angew. Chem. Int. Ed.* **45** (2006) 7674.
- [6] (a) J.N. Long, K. Kowalski, *Ferrocene containing polymers and dendrimers*. in: S. Petr (Ed.), *Ferrocene: Ligands, Materials and Biomolecules*. Wiley, Weinheim, 2008; (b) V. Chandrasekhar (Ed.), *Inorganic and Organometallic Polymers*, Springer, Heidelberg, 2005; (c) P. Nguyen, P. Gomez-Elipe, I. Manners, *Chem. Rev.* **99** (1999) 1515.
- [7] (a) G. Jaouen, N. Metzler-Nolte (Eds.), *Medicinal Organometallic Chemistry*, Springer, Berlin, 2010; (b) M. Salmann, N. Metzler-Nolte, *Bioorganometallic chemistry of ferrocene*. in: S. Petr (Ed.), *Ferrocene: Ligands, Materials and Biomolecules*. Wiley, Weinheim, 2008.
- [8] *Ferrocene ligands, part 1*. in: S. Petr (Ed.), *Ferrocene: Ligands, Materials and Biomolecules*. Wiley, Weinheim, 2008.
- [9] J. Heck, M. Dede, *Ferrocene based electro-optical materials*. in: S. Petr (Ed.), *Ferrocene: Ligands, Materials and Biomolecules*. Wiley, Weinheim, 2008.
- [10] M.L.H. Green, D.K.P. Ng, *Chem. Rev.* **95** (1995) 439.
- [11] The hafnium and tantalum complexes [(η⁷-C₇H₇)M(η⁵-C₅H₅)] were reported only recently; (a) for M = Hf, see S. Büschel, T. Bannenberg, C.G. Hrib, A. Glöckner, P.G. Jones, M. Tamm, *J. Organomet. Chem.* **694** (2009) 1244; (b) for M = Ta, see W. Noh, G.S. Girolami, *Inorg. Chem.* **45** (2008) 535.
- [12] C.J. Groenenboom, H.J. de Liefde Meijer, F. Jellinek, *J. Organomet. Chem.* **69** (1974) 235.
- [13] L.B. Kool, M. Ogasa, M.D. Rausch, R.D. Rogers, *Organometallics* **8** (1989) 1785.
- [14] M. Ogasa, M.D. Rausch, R.D. Rogers, *J. Organomet. Chem.* **403** (1991) 279.
- [15] R. Fierro, M.D. Rausch, R.D. Rogers, M. Herberhold, *J. Organomet. Chem.* **472** (1994) 87.
- [16] M. Tamm, A. Kunst, T. Bannenberg, E. Herdtweck, P. Sirsch, C.J. Elsevier, J.M. Ernsting, *Angew. Chem. Int. Ed.* **43** (2004) 5530.
- [17] M. Tamm, A. Kunst, E. Herdtweck, *Chem. Commun.* (2005) 1729.
- [18] M. Tamm, A. Kunst, T. Bannenberg, S. Randoll, P.G. Jones, *Organometallics* **26** (2007) 417.
- [19] M. Tamm, *Chem. Commun.* (2008) 3089.
- [20] C. Elschenbroich, F. Paganelli, M. Nowotny, B. Neumüller, O. Burghaus, *Z. Anorg. Allg. Chem.* **630** (2004) 1599.
- [21] H. Braunschweig, M. Lutz, K. Radacki, A. Schaumlöffel, F. Seeler, C. Unkelbach, *Organometallics* **25** (2006) 4433.
- [22] A. Bartole-Scott, H. Braunschweig, T. Kupfer, M. Lutz, I. Manners, T.-I. Nguyen, K. Radacki, F. Seeler, *Chem. Eur. J.* **12** (2006) 1266.
- [23] H. Braunschweig, T. Kupfer, M. Lutz, K. Radacki, *J. Am. Chem. Soc.* **129** (2007) 8893.
- [24] H. Braunschweig, M. Friedrich, T. Kupfer, K. Radacki, *Chem. Commun.* **47** (2011) 3998.
- [25] S.K. Mohapatra, S. Büschel, C. Daniliuc, P.G. Jones, M. Tamm, *J. Am. Chem. Soc.* **131** (2009) 17014.
- [26] H. Braunschweig, M. Fuß, S.K. Mohapatra, K. Kraft, T. Kupfer, M. Lang, K. Radacki, C.G. Daniliuc, P.G. Jones, M. Tamm, *Chem. Eur. J.* **16** (2010) 11732.
- [27] (a) H.T. Verkouw, M.E.E. Veldman, C.J. Groenenboom, H.O. van Oven, H.J. de Liefde Meijer, *J. Organomet. Chem.* **102** (1975) 49; (b) B. Demerseman, P.H. Dixneuf, *J. Organomet. Chem.* **210** (1981) C20; (c) B. Demerseman, P.H. Dixneuf, G. Douglade, R. Merier, *Inorg. Chem.* **21** (1982) 3942.
- [28] S. Büschel, A.-K. Jungton, T. Bannenberg, S. Randoll, C.G. Hrib, P.G. Jones, M. Tamm, *Chem. Eur. J.* **15** (2009) 2176.
- [29] (a) G. Wilkinson, J.M. Birmingham, *J. Chem. Soc. A* (1954) 4281; (b) P. Geymayer, E.G. Rochow, U. Wannagat, *Angew. Chem. Int. Ed.* **3** (1964) 633; (c) B.-L. Li, M.A. Goodman, R.H. Neilson, *Inorg. Chem.* **23** (1984) 1368; (d) T. Hayashi, M. Konishi, M. Kumada, *Tetrahedron Lett.* **21** (1979) 1871.
- [30] G.M. Sheldrick, *Acta. Crystallogr.* **A64** (2008) 112.
- [31] A.L. Spek, *J. Appl. Cryst.* **36** (2003) 7.
- [32] R. Broussier, A. Da Rold, B. Gautheron, Y. Dromzee, Y. Jeannin, *Inorg. Chem.* **29** (1990) 1817.
- [33] T.N. Mitchell, *J. Organomet. Chem.* **49** (1973) 189.
- [34] M. Kumar, F. Cervantes-Lee, K.H. Pannell, J. Shao, *Organometallics* **27** (2008) 4739.
- [35] D. Gourier, D. Samuel, *Inorg. Chem.* **27** (1988) 3018.
- [36] K.A. Iyssenko, M.Y. Antipin, S.Y. Ketkov, *Russ. Chem. Bull. Int. Ed.* **50** (2001) 130.
- [37] (a) M.J. MacLachlan, J. Zheng, K. Thieme, A.J. Lough, I. Manners, C. Mordas, R. LeSuer, W.E. Geiger, L.M. Liable-Sands, A.L. Rheingold, *Polyhedron* **19** (2000) 275; (b) F. Jäkle, A. Berenbaum, A.J. Lough, I. Manners, *Chem. Eur. J.* **6** (2000) 2762.
- [38] J.A. Gamboa, A. Sundararaman, L. Kakalis, A.J. Lough, F. Jäkle, *Organometallics* **21** (2002) 4169.
- [39] B. Ferber, S. Top, R. Welter, G. Jaouen, *Chem. Eur. J.* **112** (2006) 2081.
- [40] C. Elschenbroich, O. Schiemann, O. Burghaus, K. Harms, J. Pebler, *Organometallics* **18** (1999) 3273.
- [41] M. Wedler, H.W. Roesky, F.T. Edelmann, *Z. Naturforsch. B. Chem. Sci.* **43** (1988) 1461.
- [42] V. Chandrasekhar, P. Sasikumar, P. Singh, R. Thirumoorthi, T. Senapati, *J. Chem. Sci.* **120** (2008) 105.
- [43] V. Chandrasekhar, K. Gopal, S. Nagendran, P. Singh, A. Steiner, S. Zacchini, J.F. Bickley, *Chem. Eur. J.* **11** (2005) 5437.
- [44] K. Jurkschat, C. Kruger, J. Meunier-Piret, *Main Group Met. Chem.* **15** (1992) 61.
- [45] C. Glidewell, D.C. Liles, *Acta Crystallogr. Sect. B.* **34** (1978) 129.
- [46] S. Kersch, B. Wrackmeyer, D. Männig, H. Nöth, R. Staudigl, *Z. Naturforsch. B. Chem. Sci.* **42** (1987) 387.
- [47] C. Glidewell, D.C. Liles, *J. Chem. Soc. Chem. Commun.* (1979) 93.
- [48] A. Houlton, R.M.G. Roberts, J. Silver, *J. Chem. Soc. Dalton Trans.* (1990) 1543.
- [49] G. Kehr, R. Fröhlich, B. Wibbeling, G. Erker, *Chem. Eur. J.* **6** (2000) 258.

- [50] J.L. Calderon, F.A. Cotton, B.G. DeBoer, J. Takats, *J. Am. Chem. Soc.* 28 (1971) 3593.
- [51] J.L. Calderon, F.A. Cotton, J. Takats, *J. Am. Chem. Soc.* 28 (1971) 3587.
- [52] L.N. Zkharov, Y.T. Struchkov, V.V. Sharutin, O.N. Suvorova, *Cryst. Struct. Commun.* 8 (1979) 436.
- [53] K.-H. Thiele, C. Krüger, *Z. Anorg. All. Chem.* 590 (1990) 55.
- [54] W.E. Hunter, D.C. Hrcir, R.V. Bynum, R.A. Penttila, J.L. Atwood, *Organometallics* 2 (1983) 750.
- [55] F.R. Fronczek, E.C. Baker, P.R. Sharp, K.N. Raymond, H.G. Alt, M.D. Rausch, *Inorg. Chem.* 15 (1976) 2285.
- [56] A.C. McDonald, J. Trotter, *Acta. Crystallogr.* 17 (1964) 872.
- [57] C. Elschenbroich, J. Plackmeyer, K. Harms, O. Burghaus, J. Pebler, *Organometallics* 22 (2003) 3367.
- [58] J.D. Zeinstra, J.L. De Boer, *J. Organomet. Chem.* 54 (1973) 207.
- [59] C. Bolm, F.E. Hahn (Eds.), *Activating Unreactive Substrates – The Role of Secondary Interactions*, WILEY-VCH, Weinheim, 2009.